ELSEVIER

Chemical Engineering Journal 137 (2008) 231–237

Chemical Engineering Journal

www.elsevier.com/locate/cej

# Artificial neural network to predict the growth of the indigenous *Acidthiobacillus thiooxidans*

Hsuan-Liang Liu [a,b,*], Fu-Chiang Yang [a], Hsin-Yi Lin [b], Chih-Hung Huang [a], Hsu-Wei Fang [b], Wei-Bor Tsai [c], Yung-Chu Cheng [a,b]

[a] *Graduate Institute of Biotechnology, National Taipei University of Technology, 1 Sec. 3 ZhongXiao E. Road, Taipei 10608, Taiwan*
[b] *Department of Chemical Engineering and Biotechnology, National Taipei University of Technology, 1 Sec. 3 ZhongXiao E. Road, Taipei 10608, Taiwan*
[c] *Department of Chemical Engineering and Biotechnology, National Taiwan University, 1 Sec. 4 Roosevelt Road, Taipei 10617, Taiwan*

Received 29 November 2006; received in revised form 12 April 2007; accepted 22 April 2007

**Abstract**

In this study, the growth of the indigenous *Acidithiobacillus thiooxidans* was predicted using artificial neural network (ANN). Four important variables of the growth medium: $KH_2PO_4$, $(NH_4)_2SO_4$, $MgSO_4$, and elemental sulfur ($S^0$) were fed as input into the ANN model, while the dry cell weight (DCW) was the output. The ANN model adopted in this study, consisting of an input layer, a hidden layer, and an output layer, was found to give satisfactory results. Among different combinations of 10 mostly used transfer functions, Gaussian and Sigmoid transfer functions were selected for the hidden and the output layers, respectively, to minimize the error between the experimental results and the estimated outputs. Experimental data were randomly separated into a training set and a test set with 22 and 8 experimental runs, respectively. The resulting ANN shows satisfactory prediction of the DCW with $R^2 = 0.991$ and mean relative deviation (RD) = 0.026. The optimal medium composition of the indigenous *A. thiooxidans* was further predicted to be $KH_2PO_4 = 1.0$ g/l, $(NH_4)_2SO_4 = 3.5$ g/l, $MgSO_4 = 0.65$ g/l, and $S^0 = 23$ g/l with the optimal DCW being 0.722 g/l. The results of this study suggest that ANN provides a powerful tool in studying the nonlinear and time-variant biological processes.


*Keywords:* *Acidithiobacillus thiooxidans*; Artificial neural network (ANN); Elemental sulfur; Transfer function; Gaussian; Sigmoid

## 1. Introduction

*Acidithiobacillus* spp. (e.g., *Acidithiobacillus thiooxidans* and *Acidithiobacillus ferrooxidans*), playing an important role in the sulfur cycle in the biosphere, can enhance the metal bioleaching rate from sulfides. The capability of producing acidophilic conditions by utilizing energy directly from inorganic sulfur compounds allows them to be widely used in the bioleaching processes [1]. Although the advantages of bioleaching are its relatively low cost, the mild conditions of the process, and the subsequent low demand for energy or landfill space compared with conventional technologies, the kinetics of bioleaching mechanisms is still poorly understood. Moreover, to meet the industrial requirements, it is desired to harvest a large quantity of cells in the logarithmic growth phase, in which cells exhibit a relatively high growth rate and subsequently produce a relatively high amount of sulfuric acid. In other words, higher cell concentration and sulfuric acid production have to be attained in order to achieve higher bioleaching efficiency. However, *A. thiooxidans* does not grow readily, and its cell and sulfuric acid concentrations are usually very low [2]. The highest cell and sulfuric acid concentrations obtained by conventional shaking flask cultivation were about 0.224 g/l [3] and 15,000 ppm [4], respectively, in 8–11 days.

Previously, several mathematical models have been developed to predict the growth or bioleaching behaviors of *Acidithiobacillus* spp. [5–11]. However, the multiplicity of the factors taken into consideration in microbial growth or bioleaching process complicates the model development using classical statistical techniques. Thus, a satisfactory mathematical model describing the highly nonlinear behaviors of bacterial growth and bioleaching is still difficult to find [5]. In this regard, the

* Corresponding author at: Graduate Institute of Biotechnology, National Taipei University of Technology, 1 Sec. 3 ZhongXiao E. Road, Taipei 10608, Taiwan. Tel.: +886 2 2771 2171x2542; fax: +886 2 2731 7117.
*E-mail address:* f10894@ntut.edu.tw (H.-L. Liu).

1385-8947/$ – see front matter © 2007 Published by Elsevier B.V.
doi:10.1016/j.cej.2007.04.024

**Nomenclature**

| | |
|---|---|
| ANN | artificial neural network |
| $b_k$ | the bias of $k$th output neuron |
| $B_j$ | the bias of $j$th hidden neuron |
| $d$ | the total number of input neurons |
| DCW | dry cell weight |
| DOE | design of experiments |
| $D_{EST}$ | estimated values |
| $D_{EXP}$ | experimentally determined values |
| ESS | error sum of squares |
| $f$ | transfer function |
| $g$ | transfer function |
| $m$ | the total number of hidden neurons |
| $M$ | the slope of the estimated and experiment dry cell weight |
| MLP | multi-layer feedforward perceptron network |
| MSE | mean squared error |
| $n$ | the total number of the test data |
| $N_j$ | the output of $j$th hidden neuron |
| RD | mean relative deviation |
| RSM | response surface methodology |
| $S^0$ | elemental sulfur |
| $W_{i,j}$ | the weight between $i$th input neuron and $j$th hidden neuron |
| $W_{k,j}$ | the weight between $j$th hidden neurons and $k$th output neuron |
| $X_i$ | the output of $i$th input neuron |
| $Y_k$ | the output of $k$th output neuron |

regression model becomes a common practice for such systems. However, it may give erroneous results due to the wrong estimation of the regression coefficients. In contrast, approximation models such as artificial neural networks (ANNs) provide a very powerful and reliable tool for precisely predicting the optimal conditions in the complicated systems such as the nonlinear and time-variant biological processes [12].

ANN is a nonlinear estimation technique which processes information in a way that resembles the human brain. ANN learns the patterns from historical datasets and generalizes about the mathematical relationships between input variables and their corresponding output value. The main advantage of the ANN approach over traditional methods is that it does not require an explicit description of the complex nature of the underlying process in a mathematical form [13]. So far, a variety of ANNs has been investigated and applied because of their wide range of suitability for assessing all kinds of complex systems with time variant, multiple variables, and nonlinear. The applications of such networks have found their use in many aspects such as ecological and environmental sciences [14]. For example, Acharya et al. [15] have successfully predicted sulphur removal by *Acidithiobacillus* spp. using ANN. Nagendra and Khare [16] have adopted ANN to model nitrogen dioxide dispersion from vehicular exhaust emissions. In addition, Yu et al. [17] and Sarangi and Bhattacharya [18] have compared ANN with several nonlinear regression models in predicting shrimp growth and sediment loss from watershed, respectively, and their results both showed that ANN outperforms regression models for the complex set of conditions. Thus, ANN was adopted to predict the growth of the indigenous *A. thiooxidnas* using four important variables of the growth medium: $KH_2PO_4$, $(NH_4)_2SO_4$, $MgSO_4$, and elemental sulfur ($S^0$) as input in this study.

## 2. Materials and methods

### 2.1. Microorganism

The indigenous *A. thiooxidans* used throughout this study was obtained from the sewerage samples from a sulfate-contaminated site near Keelung, Taiwan [4]. The general growth medium (N:P = 5:1; compositions (g/l): $KH_2PO_4 = 1.0$, $(NH_4)_2SO_4 = 2.54$, $MnSO_4 = 0.02$, $MgSO_4 = 0.1$, $CaCl_2 = 0.03$, $FeCl_3 = 0.02$, powdered $S^0 = 5.0$, nystatin = 0.1; pH 4.0) was used to cultivate this microorganism in a water-bath shaker (110 rpm) at 30 °C. Biomass concentrations and pH level were periodically measured over the entire cultivation time.

### 2.2. Analytical methods

Aliquots of 10 ml were taken from the culture and filtered through a general grade filter paper (Advantec, Tokyo, 90 mm) to eliminate residual sulfur. Spectrophotometer at 620 nm was performed against the general gravimetric results to obtain a calibration curve. By reading the turbidity of a given sample culture, the corresponding amount of biomass was obtained ($1.00\ OD_{620nm} \cong 0.98 \pm 0.08$ g/l DCW). The absorbance was measured by DR/2000 spectrophotometer (HACH, Loveland, CO). Using pH 4.0 and 10.0 standard buffers (Fisher Scientific, Tokyo, Japan) for calibration, standard measurement of pH was undertaken by using pH electrode and meter (Cole-Parmer, Vernon Hills, IL) with an accuracy of 0.1 pH unit.

### 2.3. Experimental design

Shake flask experiments were carried out for the growth of the indigenous *A. thiooxidans* using $KH_2PO_4$, $(NH_4)_2SO_4$, $MgSO_4$, and $S^0$ as the four test variables. Experiments were performed in sterilized 500 ml Erlenmeyer flasks with 10% of isolated bacterial cultures in 150 ml of the growth medium. 30 cultivation experiments were designed and summarized in Table 1, among which 22 and 8 sets were used as the training and testing sets, respectively.

### 2.4. Artificial neural network

So far, several types of ANNs such as feedback networks and feed-forward networks have been developed. The common trait is that every network consists of several artificial neurons in each layer. In general, the first layer is the input layer used to receive information and the last one is the output layer to obtain the calculated results. Between them there are one or

Table 1
The compositions of the growth medium for the 30 experimental runs in this study, with 22 and 8 runs used as the training and testing sets, respectively

| Experimental runs | $X_1$ | $X_2$ | $X_3$ | $X_4$ |
|---|---|---|---|---|
| 1 | 0.55 | 2.0 | 0.08 | 3 |
| 2 | 1.45 | 2.0 | 0.08 | 3 |
| 3 | 0.55 | 3.0 | 0.08 | 3 |
| 4 | 1.45 | 3.0 | 0.08 | 3 |
| 5 | 0.55 | 2.0 | 0.20 | 3 |
| 6 | 1.45 | 2.0 | 0.20 | 3 |
| 7 | 0.55 | 3.0 | 0.20 | 3 |
| 8 | 1.45 | 3.0 | 0.20 | 3 |
| 9 | 0.55 | 2.0 | 0.08 | 7 |
| 10 | 1.45 | 2.0 | 0.08 | 7 |
| 11 | 0.55 | 3.0 | 0.08 | 7 |
| 12 | 1.45 | 3.0 | 0.08 | 7 |
| 13 | 0.55 | 2.0 | 0.2.0 | 7 |
| 14 | 1.45 | 2.0 | 0.2.0 | 7 |
| 15 | 0.55 | 3.0 | 0.2.0 | 7 |
| 16 | 1.45 | 3.0 | 0.2.0 | 7 |
| 17 | 0.10 | 2.5 | 0.14 | 5 |
| 18 | 1.90 | 2.5 | 0.14 | 5 |
| 19 | 1.00 | 1.5 | 0.14 | 5 |
| 20 | 1.00 | 3.5 | 0.14 | 5 |
| 21 | 1.00 | 2.5 | 0.02 | 5 |
| 22 | 1.00 | 2.5 | 0.26 | 5 |
| 23 | 1.00 | 2.5 | 0.14 | 1 |
| 24 | 1.00 | 2.5 | 0.14 | 9 |
| 25 | 1.00 | 2.5 | 0.14 | 11 |
| 26 | 1.00 | 2.5 | 0.14 | 13 |
| 27 | 1.00 | 2.5 | 0.14 | 15 |
| 28 | 1.00 | 2.5 | 0.14 | 17 |
| 29 | 1.00 | 2.5 | 0.14 | 19 |
| 30 | 1.00 | 2.5 | 0.14 | 21 |

$X_1$: $KH_2PO_4$ (g/l), $X_2$: $(NH_4)_2SO_4$ (g/l), $X_3$: $MgSO_4$ (g/l), and $X_4$: $S^0$ (g/l).

several neuron layers, the so-called "hidden layers". The most widely applied ANN is the multi-layer feedforward perceptron (MLP) network. This kind of neural network consists of three layers: a layer of input units is connected to a layer of hidden units, which is connected to a layer of output units (Fig. 1). The number of neurons in the input and the output layers depends on the respective number of input and output parameters taken into consideration. However, the hidden layer may contain zero or more neurons. The activity of the input layer represents the raw information that is fed into the network. The activity of each hidden neuron is determined by the activities of the input neurons and the weights on the connections between the input and the hidden neurons. The behavior of the output neurons depends on the activity of the hidden neurons and the weights between the hidden neurons. The weighted sums of the outputs from the input and the hidden layers are given by Eqs. (1) and (2), respectively:

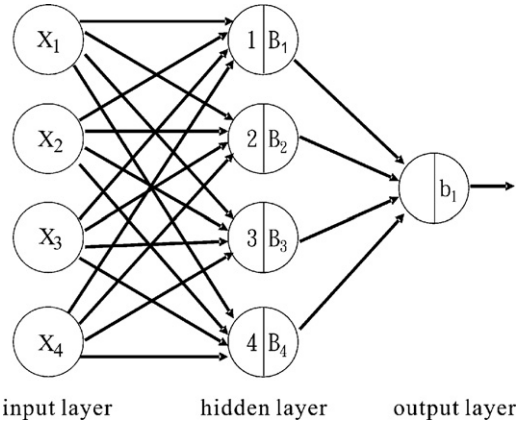


Fig. 1. Multi-layer feedforward perceptron (MLP) network model used in this study.

$$N_j = f\left(\sum_{i=0}^{d} W_{i,j}X_i + B_j\right) \quad (1)$$

$$Y_k = g\left(\sum_{j=0}^{m} W_{k,j}N_j + b_k\right) \quad (2)$$

where, $N_j$ is the output of $j$th hidden neuron, $W_{i,j}$ the weight between $i$th input neuron and $j$th hidden neuron, $X_i$ the output of $i$th input neuron, $B_j$ the bias of $j$th hidden neuron, $d$ the total number of input neurons, $Y_k$ the output of $k$th output neuron, $W_{k,j}$ the weight between $j$th hidden neurons and $k$th output neuron, $b_k$ the bias of $k$th output neuron, $m$ the total number of hidden neurons, and $f$ and $g$ are the transfer functions. In the training phase, one set of data was fed into the network at a time and the weights and bias were optimized and then the error between the experimental results and the estimated outputs was minimized.

### 2.5. Testing the ANN approach

In Fig. 1, inputs 1–4 refer to the concentrations of $KH_2PO_4$, $(NH_4)_2SO_4$, $MgSO_4$, and $S^0$. The output is the DCW of the indigenous *A. thiooxidans*. The number of the hidden neurons was obtained by trial and error method to minimize the error between the experimental and estimated results. In addition, different combinations of the transfer functions used in the hidden and the output layers also influence the error. Mean squared error (MSE) was used as the index to determine the best combination of the transfer functions used in hidden and the output layers as follows:

$$\mathrm{MSE} = \frac{\sum (D_{\mathrm{EXP}} - D_{\mathrm{EST}})^2}{n} \quad (3)$$

In this study, 10 commonly used transfer functions listed in Table 2 were screened for the hidden and the output layers. The resulting MSE values for these combinations of transfer functions are shown in Fig. 2. It reveals that the minimized MSE was obtained when the transfer functions used for the hidden and the output layers are Gaussian and Sigmoid, respectively. Finally, mean relation deviation (RD) was used to determine the prediction accuracy of the ANN model:

$$\mathrm{RD} = \frac{1}{n}\sum \left|\frac{D_{\mathrm{EXP}} - D_{\mathrm{EST}}}{D_{\mathrm{EXP}}}\right|. \quad (4)$$

Table 2
The transfer functions tested in this study

| Serial no. | Transfer function | Formula |
|---|---|---|
| 1 | Hard limit transfer function | $f(x)=\begin{cases}0, & \text{if } x<0\\ 1, & \text{if } x\geq 0\end{cases}$ |
| 2 | Symmetrical hard limit transfer function | $f(x)=\begin{cases}-1, & \text{if } x<0\\ 1, & \text{if } x\geq 0\end{cases}$ |
| 3 | Saturating linear transfer function | $f(x)=\begin{cases}0, & \text{if } x<0\\ x, & \text{if } 0\leq x\leq 1\\ 1, & \text{if } x>1\end{cases}$ |
| 4 | Symmetrical Saturating linear transfer function | $f(x)=\begin{cases}-1, & \text{if } x<-1\\ x, & \text{if } -1\leq x\leq 1\\ 1, & \text{if } x>1\end{cases}$ |
| 5 | Positive linear transfer function | $f(x)=\begin{cases}0, & \text{if } x<0\\ x, & \text{if } x\geq 0\end{cases}$ |
| 6 | Linear transfer function | $f(x)=x$ |
| 7 | Sigmoid transfer function | $f(x)=\frac{1}{1+e^{-x}}$ |
| 8 | Hyperbolic tangent transfer function | $f(x)=\frac{e^{x}-e^{-x}}{e^{x}+e^{-x}}$ |
| 9 | Triangular basis transfer function | $f(x)=\begin{cases}0, & \text{if } x<-1\\ 1+x, & \text{if } -1\leq x<0\\ 1, & \text{if } x=0\\ 1-x, & \text{if } 0<x\leq 1\\ 0, & \text{if } x>1\end{cases}$ |
| 10 | Gaussian transfer function | $f(x)=e^{-x^2/2}$ |

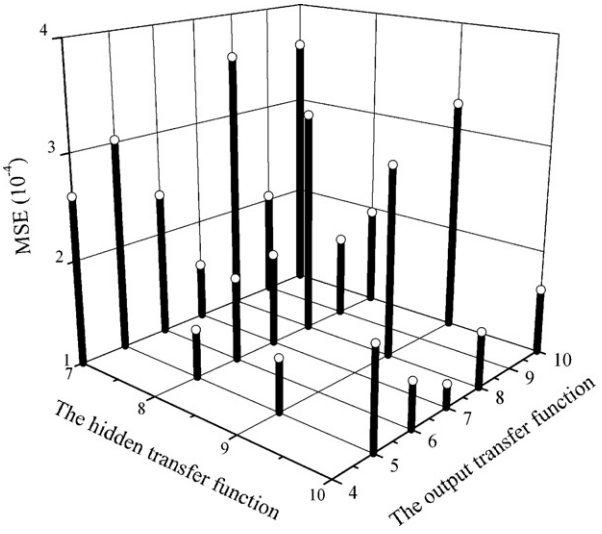


Fig. 2. The MSE values of different combinations of the transfer functions used in the hidden and output layers. The numbers in the *x*- and *y*-axis represent the serial numbers shown in Table 2. Please note that in order to clearly demonstrate that the minimized MSE value ($Z=1.22\times10^{-4}$) was obtained when Gaussian (serial no. 10) and Sigmoid (serial no. 7) transfer functions were chosen for the hidden and output layers, respectively, some MSE values of the other combinations of the transfer functions are not shown in this figure.

## 3. Results and discussion

Although ANN is a powerful tool to predict the nonlinear or time-variant systems [12], different combinations of the transfer functions used in the hidden and the output layers show significant effects on the prediction accuracy. In order to obtain the optimal combination of the transfer functions in the hidden and the output layers, trial and error method was applied to minimize the error between the estimated and experimental results. The results of the combinations of the 10 commonly used transfer functions listed in Table 2 for the hidden and the output layers in the ANN model are shown in Fig. 2. The numbers in the *x*- and *y*-axis are the serial numbers for the transfer functions given in Table 2. *z*-Axis shows the MSE values, which represent the deviations between the estimated and experimental results, for these combinations of different transfer functions. The results reveal that the minimized MSE ($Z=1.22\times10^{-4}$) was obtained when Gaussian (serial no. 10) and Sigmoid (serial no. 7) transfer functions were chosen for the hidden and output layers, respectively. Using these two transfer functions, the weights and bias for the hidden and output layers can be obtained and the results are presented in Tables 3 and 4, respectively. A total of 30 sets of data were employed in the present study, out of which 22 sets were used for training the ANN model and 8 for testing the network.

Fig. 3 shows the results of the comparison between the DCW of the indigenous *A. thiooxidans* from the experimental and estimated results in the training set. The $R^2$ value and the slope

Table 3
Weights for the hidden layer

| | Neuron number in the hidden layer | | | |
|---|---|---|---|---|
| | 1 | 2 | 3 | 4 |
| Bias in input layer | −3.7270 | 3.20977 | −6.62802 | 2.73275 |
| Input, $X_1$ | −12.1281 | 3.60308 | 12.6844 | 7.5894 |
| Input, $X_2$ | 4.87858 | 1.94767 | 20.2078 | −32.3476 |
| Input, $X_3$ | 34.3849 | 68.8834 | 4.65543 | 43.3003 |
| Input, $X_4$ | 22.5623 | −2.84966 | 1.78166 | 26.3071 |

Table 4
Weights for the output layer

| | Output |
|---|---|
| Bias in hidden layer | 0.22007 |
| Hidden layer neuron 1 | −1.50763 |
| Hidden layer neuron 2 | 20.3030 |
| Hidden layer neuron 3 | 13.6081 |
| Hidden layer neuron 4 | −16.5142 |

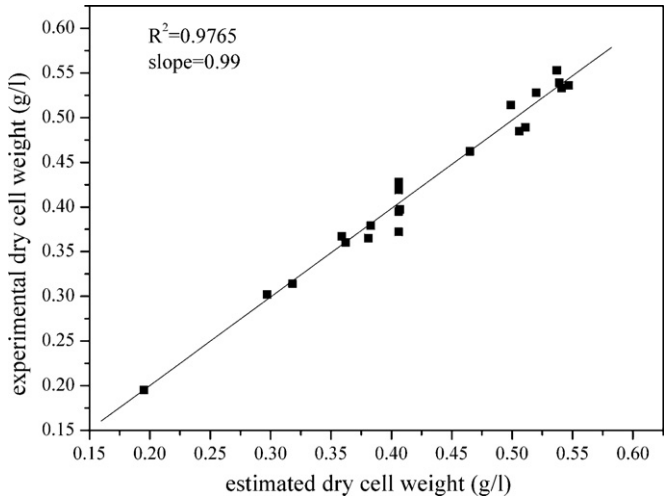


Fig. 3. Parity plot for the DCW of the indigenous *A. thiooxidans* in the training set.

between the estimated and experimental DCW are 0.9765 and 0.99, respectively, indicating that the ANN model used in this study is satisfactory. Fig. 4 gives the results of the comparison between the DCW of the indigenous *A. thiooxidans* from the experimental and estimated results in the testing set. The $R^2$ value and the slope between the estimated and experimental DCW are 0.9910 and 1.03, respectively, indicating that the ANN model could estimate the dry cell weight of the indigenous *A. thiooxidans* quite satisfactory in most of the cases, with

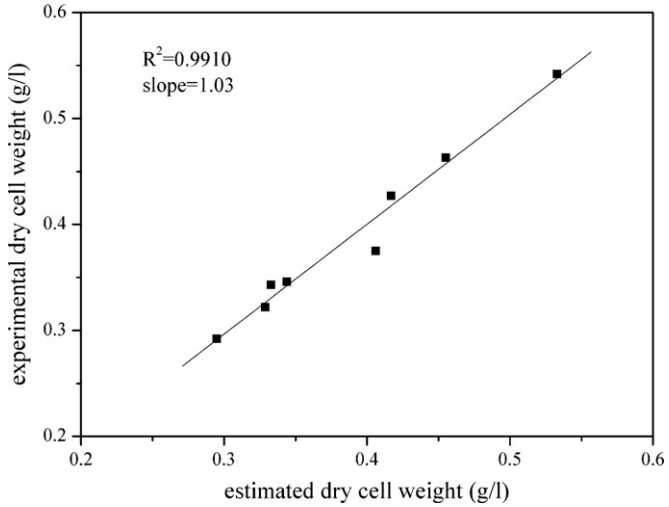


Fig. 4. Parity plot for the DCW of the indigenous *A. thiooxidans* in the testing set.

Table 5
Screening range for the optimal composition of the growth medium for the indigenous *A. thiooxidans* using the ANN model developed in this study

| | $X_1$ | $X_2$ | $X_3$ | $X_4$ |
|---|---|---|---|---|
| Minimum value | 1.0 | 3.5 | 0.65 | 15 |
| Maximum value | 3.7 | 6 | 0.80 | 45 |
| Interval | 0.1 | 0.1 | 0.01 | 1.0 |

$X_1$: $KH_2PO_4$ (g/l), $X_2$: $(NH_4)_2SO_4$ (g/l), $X_3$: $MgSO_4$ (g/l), and $X_4$: $S^0$ (g/l).

the minimum and maximum deviations between the estimated and experimental DCW being only 0.002 and 0.031 g/l, respectively. The precise prediction of the DCW the indigenous *A. thiooxidans* indicates that the ANN model used in this study is a powerful tool in predicting the nonlinear and time-variant biological processes [12].

In order to validate the ANN model used in this study in obtaining the optimal medium composition for the indigenous *A. thiooxidans*, the optimal medium composition ($KH_2PO_4$ = 3.5 g/l, $(NH_4)_2SO_4$ = 4.9 g/l, $MnSO_4$ = 0.02 g/l, $MgSO_4$ = 0.74 g/l, and $S^0$ = 23.7 g/l) obtained from our previous study using response surface methodology (RSM) [19] was further fed as input in the network. The optimal DCW estimated by RSM and ANN were 0.720 and 0.722 g/l, respectively. The optimal DCW is defined as the DCW obtained by applying the optimal medium composition, which is obtained either from RSM or ANN prediction. It is again an exhilarating result to prove the practicability of the ANN model developed in this study. However, although the ANN model developed in this study can yield very similar DCW by inputting the optimal medium composition predicted from the previous RSM experiments [19], it does not mean that the same optimized medium composition can be obtained by these two methods. To search for the optimal medium composition using the ANN model developed in this study, a variety of combination for $KH_2PO_4$, $(NH_4)_2SO_4$, $MgSO_4$, and $S^0$, was fed as input in the network. The screening range and interval of the compositions are presented in Table 5. The optimal medium composition was then obtained as $KH_2PO_4$ = 1.0 g/l, $(NH_4)_2SO_4$ = 3.5 g/l, $MgSO_4$ = 0.65 g/l, and $S^0$ = 23 g/l, with the optimal DCW = 0.719 g/l. The optimal compositions obtained using RSM and ANN were compared in Table 6. The concentrations of $KH_2PO_4$, $(NH_4)_2SO_4$, and $MgSO_4$ in the optimized medium composition determined using RSM are 3.5, 1.4, and 1.1 times, respectively, comparing to those obtained using ANN.

Table 6
Comparison of the compositions of the optimal growth mediums predicted by from response surface methodology (RSM) and artificial neural network (ANN)

| Variable (g/l) | Method | |
|---|---|---|
| | RSM[a] | ANN |
| $KH_2PO_4$ | 3.5 | 1.0 |
| $(NH_4)SO_4$ | 4.9 | 3.5 |
| $MgSO_4$ | 0.74 | 0.65 |
| $S^0$ | 23.7 | 23.0 |

[a] Data from Liu et al. [19].

However, these two methods yield very similar concentrations of $S^0$ (23.7 g/l versus 23.0 g/l) and DCW (0.720 g/l versus 0.719 g/l).

Previous contour plots obtained using RSM demonstrated that the growth of the indigenous *A. thiooxidans* is not dependent of the concentrations of $KH_2PO_4$, $(NH_4)_2SO_4$, and $MgSO_4$, whereas $S^0$ is the sole component affecting the amount of the DCW produced [19]. The non-elliptical nature of these contour plots further depicted that there is no mutual interaction between $S^0$ and each of the other three variables. The present results showing that the same optimized concentration of the elemental sulfur using different methods are in good agreement with our previous study [19]. Although the entire metabolic pathway and the nature of the multi-enzyme systems involved in the degradation of elemental sulfur are not clearly understood, the role of elemental sulfur in the growth of cells as a result of primary metabolism of the indigenous *A. thiooxidans* has been well recognized. Although elemental sulfur has been substituted with some other alternative substrate in the growth medium for the sake of cell separation and concentration measurement in the previous study [2], the amount of sulfuric acid produced was much less than the medium with elemental sulfur. It indicates that *A. thiooxidans* has the preference to utilize solid substrate as energy source. With respect to economic considerations, the optimal medium composition obtained from ANN seems to be more practical comparing to that obtained from RSM in order to produce the same amount of the DCW.

In the present study, the number of experimental data was insufficient. If a large data set is included, the accuracy of the ANN model can be further improved. Another approach would be to carry out the experiments as per design of experiment (DOE), so that the number of experiments can be dramatically reduced while retaining all the vital information of the variables under study (i.e., the effect of one parameter, two parameter interaction or even higher interactions if there are more numbers of the variables as input to the system. The ANN model developed in this study can be further used in other systems of bacterial processes with great advantages since it was observed that the DCW could be satisfactorily estimated using this model. The larger training and testing sets would greatly enhance the versatility of the resulting ANN model, which can further be used as an expert system in order to optimize the composition of the growth medium for various microorganisms within the range of the operating conditions used in the training set.

## 4. Conclusions

The most common biological models were developed from the physical and chemical principles by applying theories of mass, momentum, and energy conservation. However, such models usually fail to predict the realistic behaviors during microbial growth or bioleaching [20]. The multiplicity of factors affecting the microbial growth or bioleaching process makes it difficult for developing a practical mathematic model. In contrast, approximation models such as ANNs are very powerful and reliable in predicting the complex conditions such as nonlinear and time-variant biological processes [12]. Previous applications of ANN used for similar microbial processes include the prediction of solubilization of heavy metals from municipal sludge in batch process using *A. thiooxidans* and *A. thioparus* [21] and the prediction of metal bioleaching from municipal sludge in a continuous process using *A. ferrooxidans* [22]. In this study, we developed a three layer feed forward MLP neural network model to predict the growth of the indigenous *A. thiooxidans*. The Gaussian and Sigmoid transfer functions were selected for the hidden and output layers, respectively, with the minimal MSE ($1.22 \times 10^{-4}$). The resulting ANN model gives a satisfactory prediction of the DCW for the testing set with $R^2 = 0.991$ and RD = 0.026. We further determined the optimal composition of the growth medium for the indigenous *A. thiooxidans* as $KH_2PO_4$ = 1.0 g/l, $(NH_4)_2SO_4$ = 3.5 g/l, $MgSO_4$ = 0.65 g/l, and $S^0$ = 23 g/l, where the maximal DCW of 0.722 g/l was obtained. The present results are in accord with the previous findings suggesting that ANN is a powerful tool to study the nonlinear and time-variant biological processes [12]. However, unlike the first principle models, the ANN model, being empirical in nature, cannot be extrapolated beyond the range of the variables for which it is trained. Thus, care must be taken to use model only within this range.

## Acknowledgement

Financial support (project number: NSC 95-2622-E-027-010-CC3) from the National Science Council (NSC) of Taiwan is very much appreciated.

## References

[1] W. Krebs, C. Brombacher, P.P. Bosshard, R. Bachhofen, H. Brandl, Microbial recovery of metals from solids, FEMS Microbiol. Rev. 20 (1997) 605–617.
[2] H. Kurosawa, T. Nakagomi, K. Kanda, K. Nakamura, Y. Amano, High density cultivation of *Thiobacillus thiooxidans* S3 in a fermentor with cross-flow filtration, J. Ferment. Bioeng. 72 (1991) 36–40.
[3] R.G. Butler, Pyruvate inhibition of the carbon dioxide fixation of the strict chemolithotroph *Thiobacillus thiooxidans*, Can. J. Microbiol. 21 (1975) 2089–2093.
[4] H.-L. Liu, C.-W. Chiu, Y.-C. Cheng, The effect of metabolites from the indigenous *Thiobacillus thiooxidans* and temperature on the bioleaching of cadmium from soil, Biotechnol. Bioeng. 83 (2003) 638–645.
[5] Y.C. Chang, A.S. Myerson, Growth models of the continuous bacterial leaching of iron pyrite by *Thiobacillus ferrooxidan*, Biotechnol. Bioeng. 24 (1982) 889–892.
[6] L.S. Gormely, D.W. Duncan, R.M.R. Branion, K.L. Rinder, Continuous culture of *Thiobacillus ferrooxidans* on a zinc sulfide concentrate, Biotechnol. Bioeng. 17 (1975) 31–49.
[7] S. Asai, Y. Konishi, K. Yoshida, Kinetic model for batch bacterial dissolution of pyrite particles by *Thiobacillus ferrooxidans*, Chem. Eng. Sci. 47 (1992) 133–139.
[8] Y. Konishi, H. Kubo, S. Asai, Bioleaching of zinc sulfide concentrate by *Thiobacillus ferrooxidans*, Biotechnol. Bioeng. 39 (1992) 66–74.
[9] Y. Konishi, Y. Takasaka, S. Asai, Kinetics of growth and elemental sulfur oxidation in batch culture of *Thiobacillus ferrooxidans*, Biotechnol. Bioeng. 44 (1994) 667–673.
[10] R. Gourdon, N. Funtowicz, Kinetic model of elemental sulfur oxidation by *Thiobacillus thiooxidans* in batch slurry reactors, Bioprocess Eng. 18 (1998) 241–249.

[11] T. Kai, Y. Suenaga, A. Migita, T. Takahashi, Kinetic model for simultaneous leaching of zinc sulfide and manganese dioxide in the presence of iron-oxidizing bacteria, Chem. Eng. Sci. 55 (2000) 3429–3436.
[12] L. Ljung, System Identification-Theory for the User, New Jersey, Prentice Hall, Englewood Cliffs, 1992.
[13] K.P. Sudheer, A.K. Gosain, K.S. Ramasastri, A data-driven algorithm for constructing artificial neural network rainfall-runoff models, Hydrol. Process 16 (2002) 1325–1330.
[14] S. Lek, J.F. Guegan, Artificial neural networks as a tool in ecological modeling, an introduction, Ecol. Model. 120 (1999) 65–73.
[15] C. Acharya, S. Mohanty, L.B. Sukla, V.N. Misra, Prediction of sulphur removal with *Acidithiobacillus* sp. using artificial neural networks, Ecol. Model. 190 (2006) 223–230.
[16] S.M.S. Nagendra, M. Khare, Artificial neural network approach for modelling nitrogen dioxide dispersion from vehicular exhaust emissions, Ecol. Model. 190 (2006) 99–115.
[17] R. Yu, P.S. Leung, P. Bienfang, Predicting shrimp growth: artificial neural network versus nonlinear regression models, Aquac. Eng. 34 (2006) 26–32.
[18] A. Sarangi, A.K. Bhattacharya, Comparison of artificial neural network and regression models for sediment loss prediction from Banha watershed in India, Agric. Water Manage. 78 (2005) 195–208.
[19] H.-L. Liu, Y.-W. Lan, Y.-C. Cheng, Optimal production of sulphuric acid by *Thiobacillus thiooxidans* using response surface methodology, Process Biochem. 39 (2004) 1953–1961.
[20] M.L. Shluer, F. Kargi, Bioprocess Engineering: Basic Concepts, New Jersey, Prentice Hall, Englewood Cliffs, 1992.
[21] Y.G. Du, T.R. Sreekrishnan, R.D. Tyagi, P.G.C. Campell, Effects of pH on metal solubilization from sewage sludge: a neural-net based approach, Can. J. Civil Eng. 21 (1994) 728–735.
[22] C. Laberge, D. Cluis, G. Mercier, Metal bioleaching prediction in continuous processing of municipal sewage with *Thiobacillus ferrooxidans* using neural networks, Water Resour. 34 (2000) 1145–1156.